PHILOSOPHICAL TRANSACTIONS OF THE ROYAL SOCIETY B BIOLOGICAL SCIENCES

Space, Persistence and Dynamics of Measles Epidemics

Benjamin Bolker and Bryan Grenfell

Phil. Trans. R. Soc. Lond. B 1995 **348**, 309-320
doi: 10.1098/rstb.1995.0070

Space, persistence and dynamics of measles epidemics

BENJAMIN BOLKER* AND BRYAN GRENFELL

Zoology Department, Cambridge University, Downing Street, Cambridge CB2 3EJ, UK

SUMMARY

This paper explores the relations between persistence and dynamics in measles epidemics. Most current models, including the stochastic seasonally forced and age-structured models examined here, fail to capture simultaneously the observed dynamics and persistence characteristics of epidemics in large urban populations before vaccination. Summary measures of persistence and trienniality allow us to compare epidemics in England, New York and Copenhagen with results of non-spatial and spatial stochastic models. Spatial (metapopulation) structure allows persistence and triennial dynamics to coexist in this class of models. The spatial dynamics of measles, for which detailed spatiotemporal data are available, may serve as a useful test of ideas applicable to other epidemiological and ecological systems with an important spatial component.

1. INTRODUCTION

The recent spate of interest in nonlinear dynamics in epidemiological and ecological systems has focused on the dynamics of measles epidemics in developed countries (Olsen & Schaffer 1990; Sugihara *et al.* 1990; Rand & Wilson 1991; Drepper *et al.* 1994). To a first approximation, the biennial and triennial patterns of recurring measles epidemics in these places are equivalent to those of a seasonally forced predator–prey system (with susceptibles as prey and infective individuals as predators), driven by the annual aggregation and consequent increase in infection rate of school children.

Sustained multi-year oscillations point to the importance of seasonality in measles dynamics – seasonal forcing sustains otherwise *damped* oscillations generated by simple measles models (Soper 1929; Fine & Clarkson, 1982*b*; Olsen & Schaffer 1990) – but introduction of seasonality into models brings up the problem of *persistence* in measles dynamics. Measles exists at the edge of extinction in human populations: the disease spreads so quickly, and individuals recover so quickly, that measles can only persist in communities larger than a *critical community size* of about 250000–500000 individuals (Bartlett 1957, 1960*a*; Black 1966) (figure 1).

Although Bartlett (1960*a*) was able to obtain critical community sizes in the observed range for England and Wales in simple stochastic models *without* seasonality, addition of seasonality to stochastic models raises the critical community size necessary to allow indefinite persistence of the disease in models to unrealistic levels (Bolker 1993*b*) (figure 1).

* Current address: Department of Ecology and Evolutionary Biology, Guyot Hall, Princeton University, Princeton, New Jersey 08544-1003, U.S.A.

These results are based on models assuming (incorrectly) completely homogeneous mixing among susceptibles and infectives. In ecological systems, persistence increases with the level of heterogeneity. Metapopulation theory suggests that environmental heterogeneity – in particular, subdivision of the environment into weakly coupled discrete patches – may increase persistence under some circumstances (Huffaker 1958; Pimental *et al.* 1963; Hilborn 1975; Hassell *et al.* 1991; Adler & Nuernberger 1994). Although metapopulation theory has usually been applied to extinction of single-species, predator–prey and host–parasitoid systems, its results should apply equally to the special case of host–disease systems. Real systems rarely experience the homogeneous, mass-action mixing assumed by standard epidemic models (but see Anderson & May (1984) and May & Anderson (1984)), and these differences could be critical to the persistence and dynamics of epidemics.

Various forms of heterogeneity – age structure, genetic, social, geographic and so forth (Anderson & May 1984, 1985*a*, 1992; May & Anderson 1984) – have attracted attention in the epidemiological literature, but usually from the point of view of practical epidemiological problems such as the efficacy of vaccination programs. Where researchers have considered the effects of heterogeneity on dynamics, they have largely been interested in the transient dynamics following the onset of mass vaccination, but some recent work (Schenzle 1984; Bolker 1993*a*) has considered the effects of heterogeneity on long-term dynamics as well. Introducing age structure mitigates, but does not appear to solve, the problem of persistence (figure 1 and section 2*c*).

Other work has explored the explicit effect of spatial structure on measles dynamics (Murray & Cliff 1975; Cliff & Haggett 1988; Olsen & Schaffer 1990; Schwartz 1992). Since non-spatial structure alone does

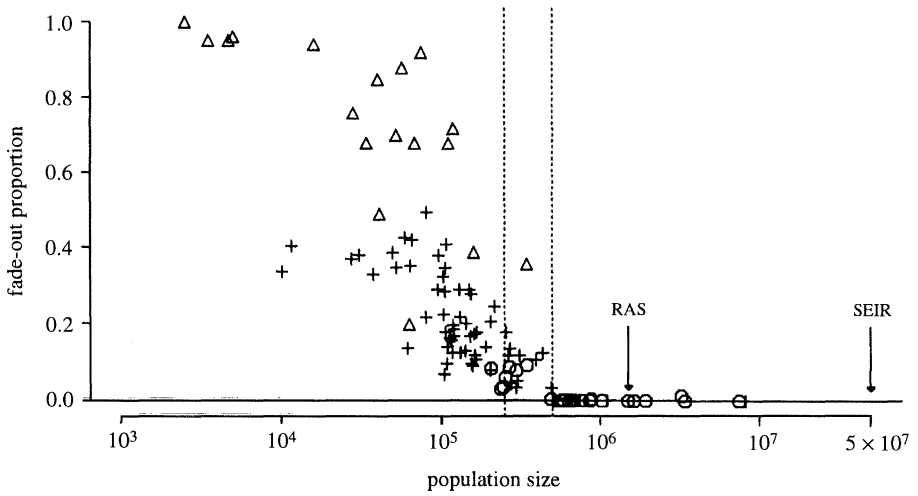

Figure 1. Empirical estimates of critical community size. Horizontal axis shows population size; vertical axis shows 'fade-out proportion', the fraction of months in each sample with no reported cases of measles. The vertical dotted lines represent the empirical estimate of critical community size range (Bartlett 1957, 1960*a*), 250000–500000. Data from Black (1966) (△, islands) Bartlett (1960*a*) (○, U.S. and Canadian cities), and Shaw (1990) (+, British cities; data originally from OPCS (1948–68)). Although there are many possible sources of variation in the data, including different reporting rates, *per capita* birth rates and levels of outside epidemiological contact, all the data fall roughly along the same curve. Arrows show the estimated critical community size for the (homogeneous) SEIR model with scaled immigration and the (age-structured) RAS model with constant immigration. Both of these models predict critical community sizes much larger than the empirical estimate (see figure 2 and section 2).

not appear to address the question of persistence (figure 2), this paper focuses on the combination of age and spatial structure, examining the relations between dynamics and persistence characteristics of spatially and age-structured stochastic models. In the process it will combine aspects of both the dynamics-oriented spatially structured models and the persistence-oriented age-structured models. The goal is to find models that are capable of replicating both the dynamics of measles and its persistence characteristics in large urban populations of developed countries.

The paper briefly reviews the observed dynamics of measles epidemics and some of the basic models current in the literature (section 2), discusses the possible importance of immigration and spatial structure to measles dynamics and examines how these factors have been incorporated in previous modelling efforts (section 3). It then briefly presents quantitative summary statistics for dynamics and persistence that allow more precise evaluation of models (section 4), defines a class of spatial measles models (section 5) and applies these statistics to the output of non-spatial and spatial measles models, showing how incorporating spatial structure in measles models can significantly alter their dynamics.

2. OBSERVED DYNAMICS AND BASIC MODELS

(*a*) *Observed dynamics*

As mentioned in the introduction, measles case reports from cities in developed countries routinely show annual (school-based) epidemics with multi-year oscillations in epidemic size. These long-term oscillations vary qualitatively from place to place and during different historical periods, ranging from regular, biennial epidemics (as seen for example in England and Wales between 1948 and 1968) to longer-period, irregular, generally triennial epidemics (as typified by the measles dynamics of Copenhagen between 1928 and 1941). (Figure 2*b* shows a time series from Copenhagen, demonstrating multi-year oscillations and a switch in the mid-1940s from triennial to annual and biennial patterns. New York City and Baltimore show similar patterns.)

Investigations of time series of measles case reports and of epidemiological models suggest that measles epidemics, if not actually undergoing chaotic dynamics, are near the edge of the chaotic regime (Ellner *et al.* 1993). The controversy over the existence of actual chaos in measles case-reporting time series continues (Sugihara & May 1990; Sugihara *et al.* 1990; Rand & Wilson 1991; Nychka *et al.* 1992; Stone 1992; Ellner *et al.* 1993; Tidd *et al.* 1993; Drepper *et al.* 1994; Grenfell *et al.* 1995). This paper will concentrate instead on a more specific comparison of models and data, the difference between biennial and triennial (or longer-period) dynamics.

(*b*) *SEIR model*

The standard SEIR model (susceptible–exposed–infective–recovered) for the dynamics of directly transmitted disease has been exhaustively analysed in the literature (Smith 1983; Aron & Schwartz 1984; Schwartz 1985; Olsen *et al.* 1988; Olsen & Schaffer 1990; Rand & Wilson 1991; Kendall *et al.* 1993; Drepper *et al.* 1994; Engbert & Drepper 1995). The basic model is

$$dS/dt = \mu(N-S) - \beta SI/N,$$

$$dE/dt = \beta SI/N - (\mu+\sigma)E,$$

$$dI/dt = \sigma E - (\mu+\gamma)I$$

PHILOSOPHICAL TRANSACTIONS OF THE ROYAL SOCIETY B BIOLOGICAL SCIENCES

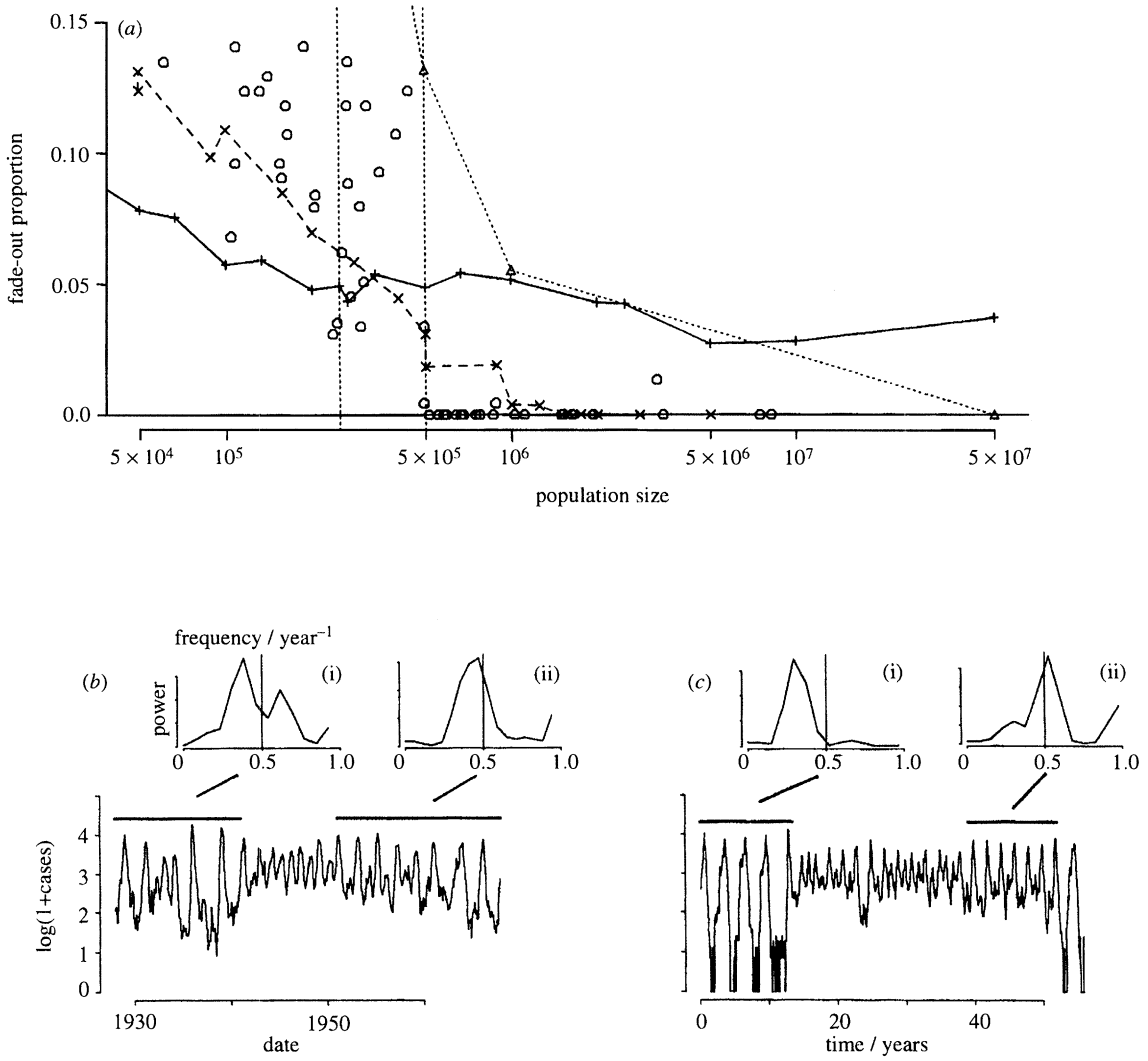

Figure 2. (*a*) Simulation estimates of critical community size. Axes as in figure 1 (note different scales). Persistence data from figure 1 are shown with open circles (○). Also shown are simulation results from the sinusoidally forced Monte Carlo SEIR model (parameters as in Olsen *et al.* (1988): $\mu = 0.02$ year^{-1}, $\beta_0/N = 0.0010107$ infective^{-1} year^{-1}, $\beta_1 = 0.28$, $\sigma = 35.84$ year^{-1}, $\gamma = 100.0$ year^{-1}) with a constant immigration rate of 21 infectives per year (+); Monte Carlo SEIR simulations with immigration proportional to population size (equal to $(2.1 \times 10^{-5})\,N$ (Olsen *et al.* 1988; Bartlett 1957)) (△); Monte Carlo RAS simulations with constant immigration rate of 21 infectives per year (parameters as in Bolker & Grenfell (1993)) (×). (*b*) Monthly measles cases from Copenhagen, 1928–64 (corrected for under-reporting, logarithmic scale). *Insets* show power spectra (smoothed with a three-point running mean) for shorter periods indicated by horizontal bars; horizontal axes show frequency per year, vertical axes give normalized power. The vertical line at 0.5 cycles per year shows the position of biennial cycles: peaks to the left of this line represent lower-frequency, longer-period cycles. (i) Triennial dynamics, 1928–41. (ii) Biennial dynamics, 1952–64. (*c*) Monthly measles cases from a Monte Carlos RAS simulation ($N = 10^8$, other parameters as in (*a*)). Insets are power spectra as in (*b*). (i) Triennial dynamics, 0–12. (ii) Biennial dynamics, 38–52. Note fade-outs in the triennial domain (i).

and

$$N = S + E + I + R. \qquad (1)$$

In these equations μ represents the *per capita* birth and death rate, $1/\sigma$ is the average latent period, and $1/\gamma$ is the average infectious period. The key epidemiological parameter in the model is the *contact rate* β, the effective rate at which infective individuals encounter and infect susceptible individuals. Addition of an annual sinusoidal variation in the contact rate, $\beta = \beta_0(1 + \beta_1 \cos 2\pi t)$, to mimic observed changes in the contact rate caused by aggregation of children in schools leads to the *sinusoidally forced* SEIR model.

(*c*) *RAS model*

A more realistic, age-structured (RAS) measles model (Bolker 1993*a*; Bolker & Grenfell 1993), first proposed by Schenzle (1984), takes the basic epidemiological structure of the SEIR model and adds age structure and a more realistic seasonal pattern to it. The age structure divides the population into four age classes – pre-school children (0–6 years), primary school children (6–10 years), adolescents (10–20 years) and adults (20 years and older) – among which epidemiological mixing takes place at different rates. The basic structure of the model remains the same, although each epidemiological category (S, E, I) is

divided into annual cohorts, each of which falls into one of the age classes. Newborns enter the first age class; the *per capita* death rate is zero until age 20 and a non-zero constant thereafter. Latency and recovery are independent of age. Children move through the age classes in one-year cohorts, which advance suddenly at the beginning of each school year to mimic the school groupings of children. As discussed by Bolker (1993*a*), seasonally forced, age-structured SEIR-based models can generally be described by an equation of the form

$$\frac{\mathrm{d}I(a)}{\mathrm{d}t} = \sum_{a'} \{[\beta_0(a,a') + f_{\mathrm{seas}}(t) \times \beta_\Delta(a,a')]\, I(a')\}\, S(a). \quad (2)$$

Here $I(a)$ and $S(a)$ are the numbers of infectives and susceptibles in age class a; $\beta_0(a,a')$ describes the baseline mixing pattern between age classes a and a'; $\beta_\Delta(a,a')$ describes the changes caused by seasonal forcing; and $f_{\mathrm{seas}}(t)$, a function mapping the time of year onto $[0,1]$, describes the pattern of seasonal change. In this case the seasonal function f_{seas} is a simple step function (0 during vacations and 1 during the school year) and $\beta_\Delta(a,a')$ is non-zero only for primary-school children. This structure allows higher mixing rates within the primary school age class during the school term than during vacations.

(*d*) *Model behaviour: dynamics*

The sinusoidally forced SEIR model exhibits an extremely broad spectrum of dynamical behaviour ranging from regular annual cycles to chaos (in this case represented by two- to six-year quasi-cycles with highly irregular phase and amplitude) (Aron & Schwartz 1984; Olsen & Schaffer 1990), depending on the amplitude of seasonal forcing. In addition, in most of the chaotic regime the sinusoidal SEIR model exhibits episodes of alternating biennial and triennial behaviour (Kendall *et al.* 1993; Schaffer *et al.* 1993), possibly matching those seen in the data.

The RAS model closely fits the observed biennial pattern of measles epidemics in England and Wales (Bolker & Grenfell 1993; Schenzle 1984) and also predicts post-vaccination measles dynamics more accurately than do homogeneous age-structured models (Schenzle 1984); it is also much more dynamically stable than the SEIR model. Over a wide range of seasonal forcing amplitudes, where the SEIR model produces irregular, chaotic dynamics with long (three- to six-year) periods, the deterministic RAS model always generates regular cycles and rarely produces cycles longer than two years. The apparent mechanism behind this behaviour is the buffering effect of children in the pre-school age class, who experience a smaller and more constant force infection than primary-school children and thus provide a reservoir of susceptibles (and infectives) to keep the system from experiencing violent swings in measles incidence (Bolker 1993*a*; Stone 1993). On the other hand, stochastic simulations of the RAS model can generate the same kinds of irregular and episodic dynamics seen in the data and in the forced SEIR model (Bolker & Grenfell 1993) for moderate-sized populations (figure 2*c*).

(*e*) *Model behaviour: persistence*

Simple SEIR models with seasonal forcing fail spectacularly in predicting the correct critical community size. In deterministic models the size of the infective class routinely falls to 10^{-10} of the total population size, which suggests that the disease would normally go extinct even in extremely large populations. Stochastic simulations reinforce this view: even when allowance is made for a fairly large immigration of infectives from outside the modelled population, measles periodically goes extinct in model population sizes of up to 50 million (see section 3 and figure 2).

Although the stochastic RAS model is less susceptible than forced SEIR models to 'fade-outs' (periodic extinctions) of disease, it still overestimates the critical community size at *ca.* 1–2 million, even when a small amount of outside immigration is allowed. Both the forced SEIR and the RAS models fail to capture the observed persistence behaviour of measles in real communities, although the RAS model comes much closer, missing the mark by a factor of two to four rather than by two orders of magnitude (figure 2*a*).

3. EFFECTS OF IMMIGRATION AND SPATIAL STRUCTURE

Many factors affect measles persistence, both in the real world and in models. Forced SEIR models in particular tend to be structurally unstable, and so any of a number of small changes in parameter values, distributions of latent or infectious periods, super- or sublinear terms in the infection rate, etc., could allow some variant of either the SEIR or RAS models to predict the empirically determined critical community size.

A useful category of explanations involves the effect of space and population structure on epidemic dynamics. Since finite persistence is the result of closed, finite populations, any attempt to deal with persistence leads immediately to questions about the definition and demarcation of a population.

(*a*) *Immigration*

For example, a typical way of dealing with fade-outs in measles models is to recognize that human communities are not really closed systems. Researchers have modelled open populations by adding a term for the immigration of infectives into the system (Bartlett 1960*b*; Griffiths 1973; Anderson & May 1986; Olsen & Schaffer 1990; Rand & Wilson 1991) or, equivalently, assuming contact of susceptibles with a constant pool of infectives outside the population (Engbert & Drepper 1995).

This modification has been used in an *ad hoc* manner for some time (Olsen & Schaffer 1990; Rand & Wilson 1991), primarily because it gets around the practical nuisance of having to re-start a simulation after every fade-out. Researchers have usually overlooked the fact that, even with a small level of immigration, forced SEIR models experience frequent fade-out and still fail to predict the empirical critical community size (figure 2).

PHILOSOPHICAL TRANSACTIONS OF THE ROYAL SOCIETY B BIOLOGICAL SCIENCES

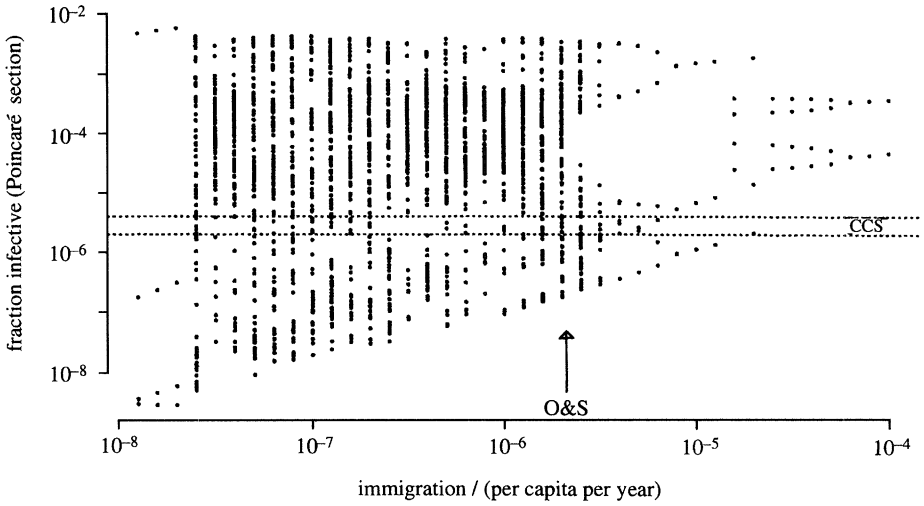

Figure 3. Bifurcation diagram of the (deterministic) sinusoidally forced SEIR model with different amounts of infective immigration. Model parameters as in figure 2. Horizontal axis shows outside epidemiological contact, as measured by the number of infectives immigrating to the population (*per capita* per year, logarithmic scale); vertical axis shows the Poincaré section of the fraction of infectives in the population (on a logarithmic scale), i.e. annual samples of infectives at the beginning of each model year. Note the sensitivity of the cynamics to small changes in the immigration parameter. Arrow indicates the immigration parameter used by Olsen *et al.* (1988), 21 infectives per year in a population of 10^6. Horizontal dashed lines show the cut-off value of one infective in the entire population for the critical community size (CCS) range of $N = 250000$–500000. (See also the elegant paper by Engbert & Drepper (1994) on this topic.)

A second, more serious problem is the extreme sensitivity of forced SEIR dynamics to differing levels of immigration (Engbert & Drepper 1994) (figure 3).

Given this sensitivity, the near impossibility of determining the actual immigration level from empirical data and the assumption (for example) that all measles epidemics in the 'outside world' are out of phase and thus generate a constant, non-seasonal flow of infective immigrants become troublesome. The true dependence of immigration rate on population size is unknown; over some range immigration rates should increase with population size, but in very large populations immigration should saturate and perhaps even decrease (as the population reaches natural boundaries, for example the boundaries of an island or continent). The extreme assumptions of constant immigration rate and immigration rate proportional to population size are both unrealistic, but constant immigration rate gives a reasonable qualitative fit to persistence data (figure 2) and is used hereafter.

(*b*) *Explicit spatial structure*

What about the dynamics of more explicitly spatial models? While many spatial epidemic models have focused on equilibrium properties (Anderson & May 1984; Sattenspiel & Dietz 1995), there has been a notable tradition of exceptions covering a variety of aims and degrees of realism. Bartlett (1960*a*), and later Grenfell (1992), studied the dynamics of simple numerical models of cities subdivided into several parts or into grids. In the 1970s and 1980s, Cliff and a variety of collaborators worked on the study of measles as a geographical diffusion process, culminating (from the point of view of this paper) with a geographically realistic (although non-seasonal, non-age-structured) spatial Monte Carlo model of epidemics in Bristol and the communities surrounding it (Murray & Cliff 1975). More recently, some researchers (Boccara & Cheong 1992, 1993; Kleczkowski & Grenfell 1995) have studied the effect of localized interactions on epidemic dynamics using cellular automaton models.

Most relevantly for this paper, Schwartz (1992) has explored a two-compartment spatial model that generates chaos by weakly linking one small and one large population, neither of which is independently chaotic. Schwartz also considers the ability of long-period dynamics to persist in finite populations. Unfortunately, he uses only deterministic models, assuming that epidemic cycles where a minimum of $1/N$ of the population is infective can survive in populations of size $\geqslant N$. In stochastic models, demographic stochasticity will probably become important when infective numbers become small, allowing fade-out even in models whose deterministic counterparts never have $I < 1/N$. Nevertheless, Schwartz's conclusion that spatial structure may drive the observed dynamics of measles epidemics is important.

There is a qualitative difference between the dynamic effects of spatial structure (or other equivalent forms of heterogeneity such as social or school structure) and simpler factors such as immigration. At the crudest level, the effect of adding immigration or making other changes to ensure persistence in *non*-spatial models is to stabilize the dynamics, filling in the troughs of an epidemic and suppressing chaos by damping the 'boom-and-bust' cycle (Berryman & Millstein 1989). Ensuring persistence tends to make chaos and long-period, usually triennial, cycles less likely; this negative correlation between persistence and triennial dynamics applies to a wide range of non-spatial compartmental measles models (see, for example: Bolker 1993*a*; Stone 1993). Although many non-spatial models may be fixed to give the correct

PHILOSOPHICAL TRANSACTIONS OF THE ROYAL SOCIETY B BIOLOGICAL SCIENCES

critical community size by adjusting immigration or other parameters, it can only be at the expense of triennial or longer-period cycles. The rest of this paper considers when and how spatial models of measles epidemics can simultaneously capture the long-period epidemics and the persistence criteria observed in the real world.

4. QUANTIFYING PERSISTENCE AND DYNAMICS

The previous section claimed that triennial dynamics and persistence cannot coexist in non-spatial measles models. Do they coexist in the real world? Cities such as Copenhagen, New York and Baltimore do not experience fade-out in the twenty- to forty-year time spans observed, and appear to have triennial dynamics at times; this section will develop more quantitative measures of persistence and periodicity to show that non-spatial compartmental measles models really fail to reproduce observed epidemic patterns.

(*a*) *Summary statistics for persistence and dynamics*

The *fade-out proportion*, the proportion of months in a data series or in a simulation with no reported cases of measles, quantifies persistence well. (Other statistics, such as the number of fade-out periods of a given length or number of years without a fade-out, characterize slightly different aspects of persistence patterns; most of the statistics give similar results except in extreme cases.) Sometimes, long simulations will have a non-zero but very small fade-out proportion. If the fade-out proportion for a particular simulation run represents less than one month of fade-out in the entire forty-year time span reported for Copenhagen (the longest available data series), it is below the *resolution limit* and can be considered consistent with the observed data sets that show persistence.

Standard spectral analysis techniques (Chatfield 1975) reveal the relative importance of two- and three-year epidemic cycles in a given simulation or data series. The area underneath particular peaks in the (smoothed) power spectrum of measles case reporting data gives a measure of the biennial or triennial nature of the epidemics.

The most useful summary statistic is the *power ratio*, defined as the ratio of the triennial power (area under the triennial part of the power spectrum, around a frequency of 0.33 year^{-1}) to the biennial power (area under the biennial part of the power spectrum, around a frequency of 0.5 year^{-1}) (figure 4). The power ratio is a single number that quantifies the patterns of interest (in this particular case) in the power spectrum.

(*b*) *Comparing real and simulated epidemics*

The fade-out proportion and power ratio can be used to compare a variety of real and simulated epidemics, confirming the problem: while measles persistence and irregularity (triennial epidemics) ap-

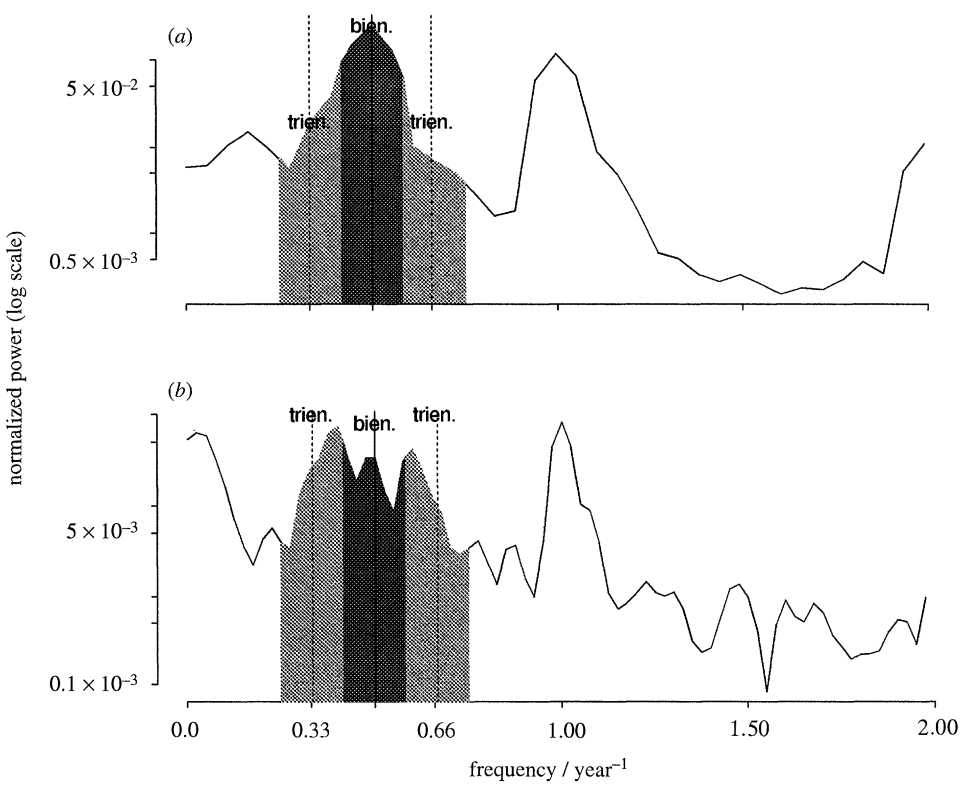

Figure 4. Power spectra and power bands for the data sets from (*a*) England and Wales (1948–66) (p.r. 0.089) and (*b*) Copenhagen (1928–64) (p.r. 1.27). Figures show the power spectra of the data, Fourier transformed and smoothed with a three-point running mean. Light shading indicates the power associated with triennial epidemics, with frequency ranges 0.253–0.413 year^{-1} and 0.583–0.743 year^{-1}; dark shading indicates the power associated with biennial epidemics, with frequency range 0.413–0.583 year^{-1}.

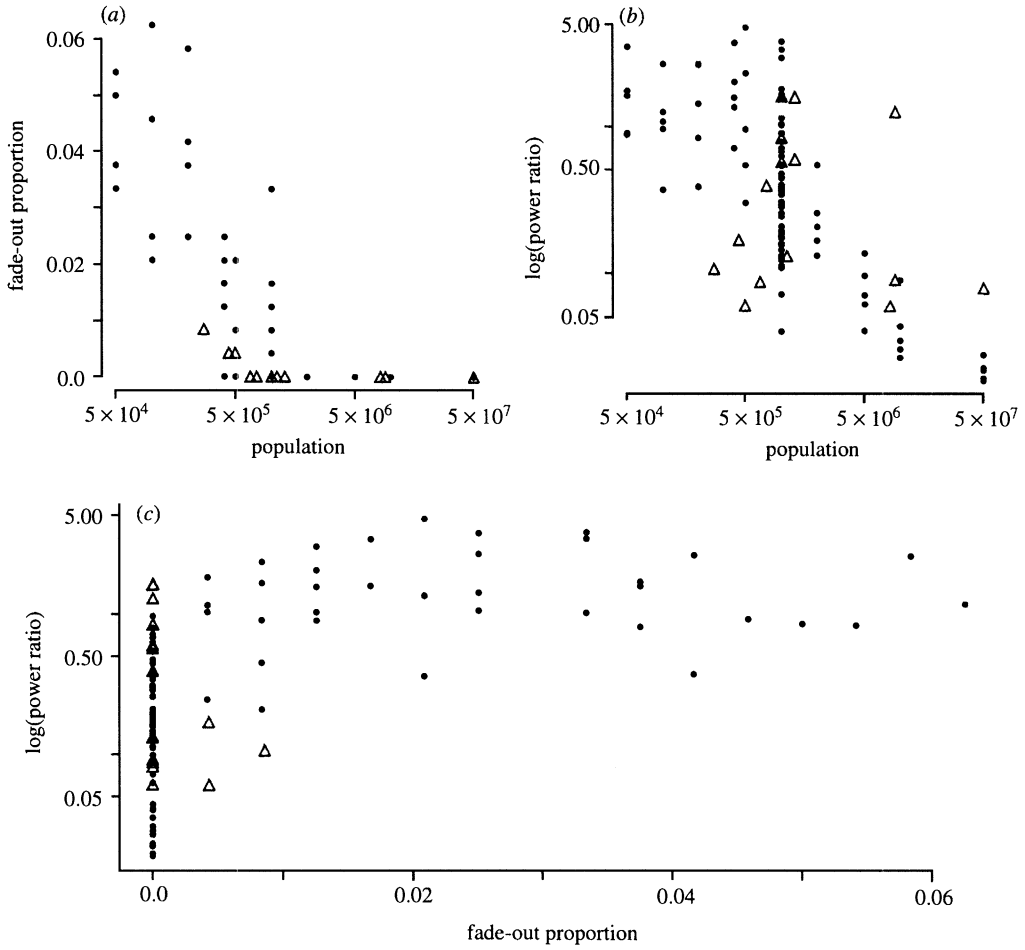

Figure 5. Plots of power ratio, fade-out proportion and population size for the Monte Carlo RAS model (●) and measles data from England and Wales, New York, Copenhagen and Baltimore (△). (*a*) Fade-out proportion (vertical axis) versus population size (horizontal axis, logarithmic scale). (*b*) Log (power ratio) versus population size. (*c*) Log (power ratio) versus fade-out proportion. Note particularly the upper two triangular points at a fade-out proportion of zero, above all power ratios recorded for simulations where measles persisted.

pear compatible in some of the data, they cannot be reproduced together by simulations.

As mentioned above (section 2*d*), one of the characteristics of seasonally forced epidemic models is their ability to switch episodically between qualitatively different types of dynamics (figure 2) (Schaffer *et al.* 1993). Although this behaviour is fascinating from a theoretical point of view, perhaps representing an instance of intermittency (Grebogi *et al.* 1983; Schaffer *et al.* 1993), and perhaps reflected in the shifts in measles dynamics in Copenhagen and New York in the 1940s and 1950s, it becomes a nuisance when trying to compare simulations with data. Because of the way that the fade-out proportions and power ratios average among different episodes, a century of simulation output containing an 80-year episode of biennial dynamics and zero fade-out and a twenty-year episode of triennial dynamics and high fade-out could appear, when aggregated, to be a century of triennial dynamics with negligibly low fade-out. To avoid this problem, all simulation results have had fade-out proportions and power ratios calculated for each twenty-year block separately. Similarly, the data sets for Copenhagen, New York and Baltimore are broken up into several separate periods that display uniform dynamics (Copenhagen 1928–41 (triennial), 1941–52 (annual), 1952–64 (biennial); New York 1928–45 (triennial), 1945–64 (biennial); Baltimore 1928–53 (triennial), 1953–64 (biennial)).

Figure 5 shows the trends of power ratio and fade-out proportion with increasing population size in the Monte Carlo RAS model and the correlation between the two summary statistics. As population size increases, increasing the number of infectives present during troughs and thereby decreasing demographic stochasticity, the fade-out proportion and power ratio simultaneously decrease. The overall trend is from triennial epidemics with fade-outs in the troughs (high power ratio, high fade-out proportion) to biennial epidemics where measles persists during the troughs (low power ratio, zero fade-out proportion). Figure 5*c* shows the statistics for some of the available measles data sets as well as for the RAS model, indicating in particular that there are cities with persistent measles (zero fade-out) where the power ratio achieves levels higher than in any of the simulations with persistent measles.

Figure 6 summarizes the significant pattern of figure 5, showing histograms of data sets and simulations with zero fade-out or with fade-out less than the resolution limit (see above, section 4). The histogram includes simulation output from RAS model runs with popu-

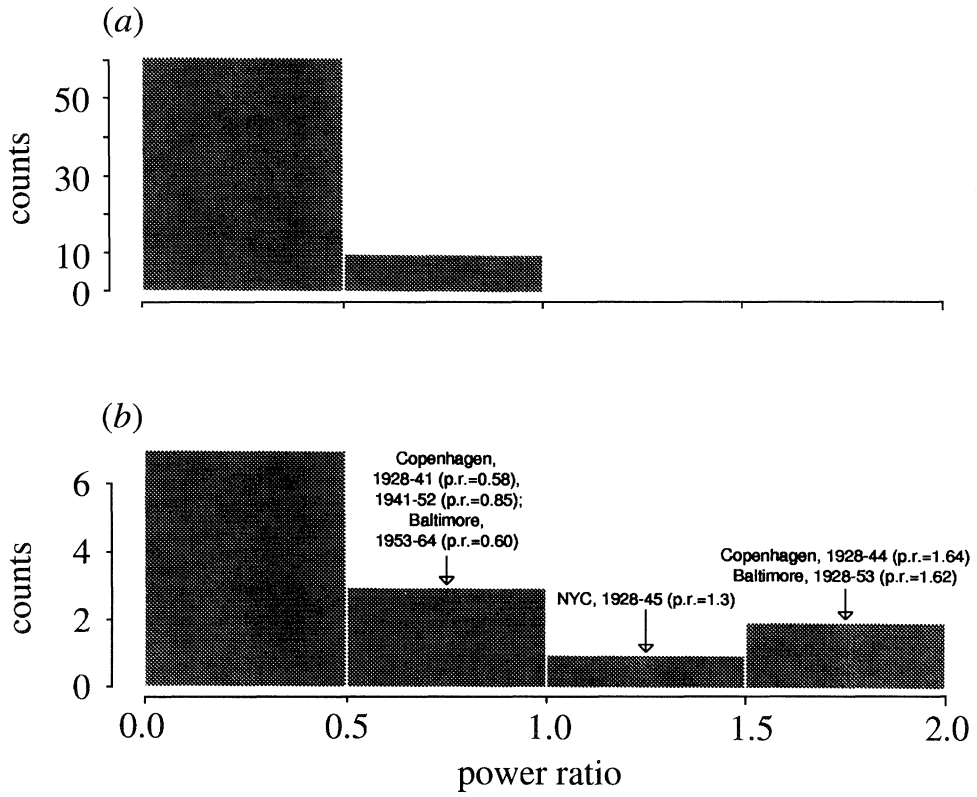

Figure 6. Histogram of power ratios for approximate twenty-year periods of (*a*) simulation ($n = 71$) and (*b*) data ($n = 13$) with zero fade-out or with fade-out less than the resolution limit (see text). Simulation runs include varying population sizes from 10^4 to 5×10^7; real data include case reports from Copenhagen, New York, English cities and London boroughs. The data distribution has a tail with power ratio greater than 1.0 that is not matched by the simulations.

lations of 50 000–50 million; similar results are obtained by changing seasonality or infective immigration rates in the RAS model. While most of the persistent simulations have power ratios less than 0.5, several of the real data sets have power ratios ranging from 0.5 to 2.0. Real cities, but not the model cities presented here (which are the most realistic extant models in this respect), can sustain triennial epidemics without fade-out.

5. SPATIAL MODELS

(*a*) *Model structure*

The simplest way to make a spatial analogue of the Monte Carlo RAS model is to impose a *patch* or *metapopulation* structure on top of the existing epidemiological and age-structured compartments. Metapopulation models take the age cohorts in the RAS model and subdivide them further into cohorts in different spatial regions, representing different cities or different boroughs or suburbs within the same metropolis. There is no explicit movement between cities, but individuals in each region have epidemiological contact with individuals in every other region.

The extension of the basic SEIR/RAS framework to multiple patches is straightforward. The basic expression for the infection rate of susceptibles of age a in city i is $\Sigma_{a'} \Sigma_j \beta_{ij}(a, a', t)\, S_i(a)\, I_j(a')$; most of the structure of a particular model lies in the definition of the β (contact) matrix. here it is defined as

$$\beta_{ij}(a, a', t) = \phi_{ij}(a, a', t)\, \beta_0(a, a', t), \qquad (3)$$

where β_0 is the contact rate as defined in the RAS model. The contact rate between a susceptible of age a in city i and an infective of age a' in city j at time t equals a multiplicative coupling factor ϕ times the effective contact rate if the two were in the same location.

Clearly, a great deal of complicated structure about the movements of children and adults at different times of year can be built into this equation (Sattenspiel & Dietz 1995). All of the results presented here will deal with a simple homogeneous-coupling case where a single coupling ϕ applies between all cities in the system, regardless of age or season ($\phi_{ij} = \phi (i \neq j)$, $\phi_{ii} = 1$). Intuitively, ϕ is the ratio of between- and within-city contacts; if $\phi = 0.01$, the probability of contact with a foreigner is 1% of the probability of local contact. (In addition, all contact rates are divided by $1/(1 + n\phi)$, where n is the number of patches, so that the total effective contact rate remains constant with increasing numbers of patches; $\phi = 1$ implies homogeneous mixing.) All patches have identical demographic and epidemiological parameters, which is unrealistic but parsimonious.

These simplest possible spatial models are used in part because of the difficulty of parameterizing even simple subdivided measles models from data. There is no accepted way of quantifying epidemiological couplings between different regions. Earlier work on spatial measles models has used either a range of coupling parameters (Bartlett 1960*a*; Grenfell 1992), parameters estimated by trial and error from simu-

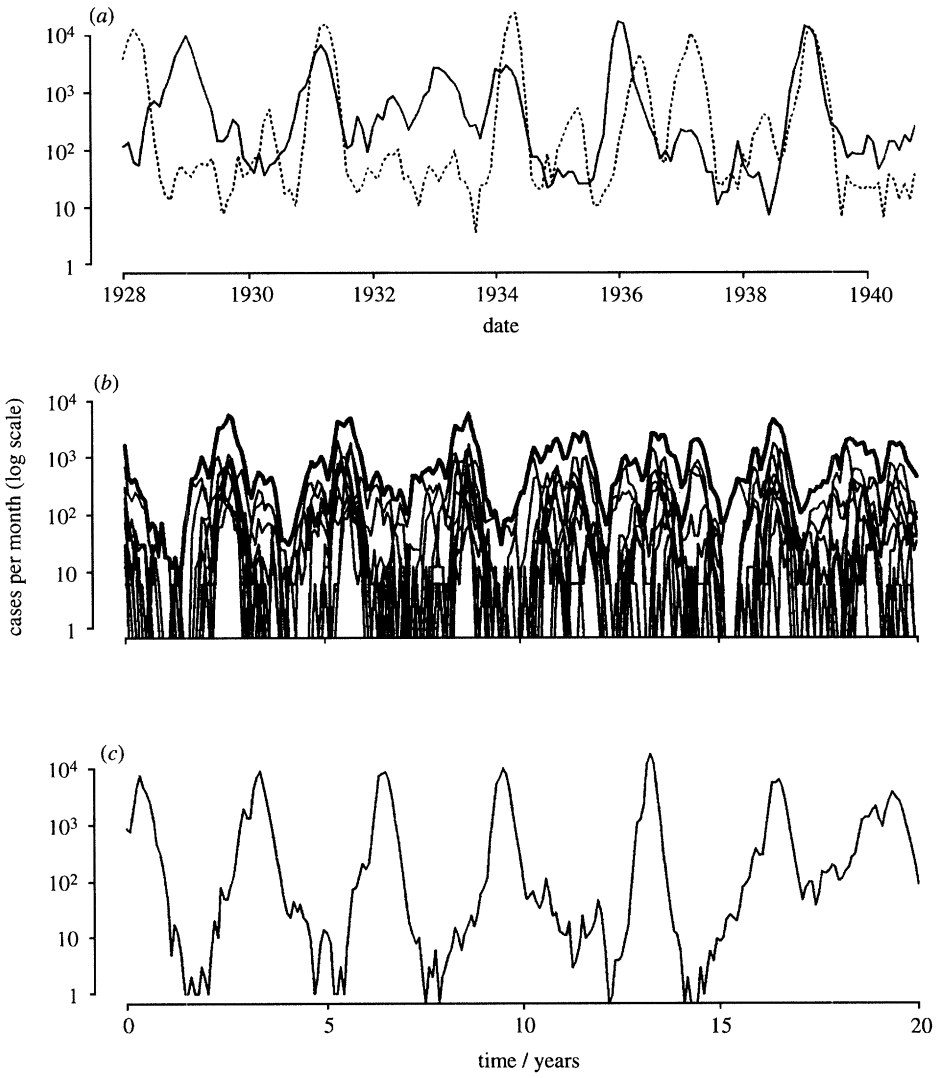

Figure 7. Triennial dynamics sampled from (*a*) Copenhagen (solid line) and Baltimore (dashed line) data sets (corrected for under-reporting), (*b*) a spatial model ($N = 10^6$, $n = 10$, $\phi = 10^{-3}$), (*c*) a non-spatial model ($N = 10^6$). Horizontal axis shows date or time in years; vertical axis shows total cases reported per month (approximated from infective time series in (*b*)) on a logarithmic scale. In (*b*), the thick upper line shows the total number of reported cases from the entire population and the thin lines show the cases from the ten subpopulations; note that the epidemics are poorly correlated among the subpopulations and that the total population is rescued from fade-out by one or two subpopulations on several occasions. In (*a*), min = 7, max = 17730 (Copenhagen), and min = 4, max = 24052 (Baltimore); in (*b*), min = 6, max = 5816; (*c*) min = 0, max = 18299.

lations (Murray & Cliff 1975) or parameters chosen by intuition (Schwartz 1992). Although recent work by Sattenspiel & Dietz (1995) has suggested some ways of quantifying epidemiological coupling by measuring human mobility patterns, their methods require specific data that is not easily available for any areas with persistent measles epidemics. Estimates based on their work (Bolker 1993*b*) suggest that 10^{-4}–10^{-1} is a plausible range for epidemiological couplings. This encompasses the range of couplings used in simulations cited above and so is not useful for distinguishing among them, but it at least makes the link between a range of mobility patterns (frequency and length of visits between cities) and a range of epidemiological coupling constants.

Another possible method for estimating coupling relies on back-estimation from the observed case reports, analogous to the Fine & Clarkson (1982*a*) estimates of seasonal variation in contact rates or the Anderson & May (1985*b*) estimates of age-structured mixing rates. If we assume homogeneous mixing within every compartment and specify some simplified contact structure (such as the single between-city contact rate used above), and if we can estimate the number of susceptible individuals in each population, contact rates may be found simply by solving a linear equation. Susceptible population sizes can be estimated by accounting for births, deaths and infections (Cliff & Haggett 1988; Fine & Clarkson 1982*a*; Grenfell *et al.* 1993, 1995), and so this method can work in theory, but preliminary attempts along these lines have run into problems with the strong correlation between cities (which reduces the amount of available information on cross-coupling).

More statistically sophisticated methods may work: time-series methods such as the Kalman filter (Kalivianakis *et al.* 1994; Cliff & Haggett 1988) are a more rigorous approach to time-varying coupling

constants. Finally, in the rare cases where highly detailed case reports are available (Becker & Wang 1993), maximum likelihood estimation can determine *all* of the relevant contact rates. However, data of this quality are extremely unusual.

The simulations reported here use a population of 10^6, in the critical community size range for the RAS model, broken up into $n = 5$, 10 or 15 equal partitions, with coupling ϕ of 10^{-4} to 10^{-1}. This range of parameters should give preliminary evidence about the ability of spatial models to overcome some of the discrepancies between persistence and dynamics observed in the SEIR and RAS models.

(*b*) *Results of spatial simulations*

The simulations show that spatial structure can enhance persistence, and that it can generate new kinds of dynamic behaviour. Figure 7 shows samples of triennial dynamics (numbers of cases reported monthly over time) from the Copenhagen data set, from a non-spatial model ($N = 10^6$) and from a spatial model ($N = 10^6, n = 10, \phi = 10^{-3}$). Both the spatial and non-spatial models generate three-year cycles, but measles fades out (and is reintroduced by infective immigration) in the epidemic troughs of the non-spatial model, while it remains persistent in Copenhagen and in the spatial model. The correlations between epidemics in the subpopulations are fairly weak in the example from the spatial model, but remain strong enough (because of similar epidemic dynamics driven by similar school calendars) to preserve a three-year cycle in total case numbers. At other periods in the same spatial simulation when the subpopulations are more highly correlated, the dynamics resemble those of the non-spatial model, with sharper epidemics and more fade-outs.

Neither the non-spatial nor the spatial model is a perfect match for the dynamics observed in Copenhagen and Baltimore. The epidemic troughs of the spatial model approximate the troughs of the data, but the non-spatial model does a better job matching the epidemic peaks of the data, and the real epidemics have even larger maxima than in the non-spatial model. In addition, the relatively poor correlations between the subpopulations (Pearson's r applied to $\log(1 + \text{cases}) = 0.33$), which allow the persistence of measles, are somewhat lower than the correlations between either the largest cities in England and Wales ($r = 0.59$ for the period 1948–66) or the boroughs within the city of London ($r = 0.69$ for 1950–59). The actual social and spatial structure that can allow urban populations to have such large epidemic peaks, be internally coherent and still maintain chains of infection in the troughs remains a puzzle. Nevertheless, as shown in figure 8, the spatial model does address the most striking qualitative problem of the non-spatial models, the negative correlation between persistence and triennial/irregular dynamics.

The model dynamics shown in figure 7 are only one example of simulated dynamics. To match the frequency of occurrence of persistent, triennial dynamics in spatial and non-spatial simulations against the data,

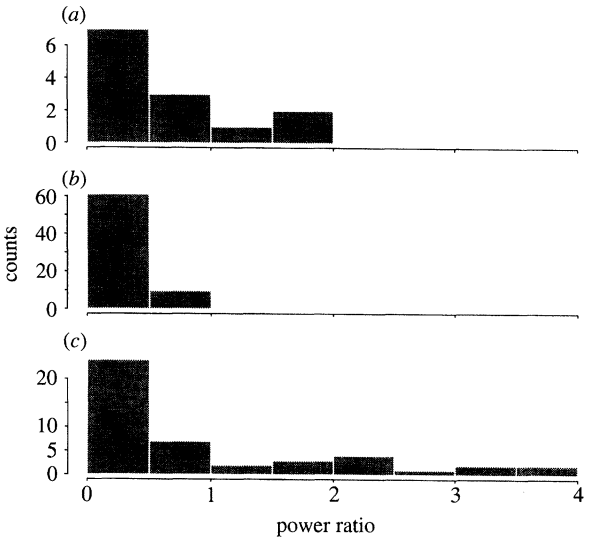

Figure 8. Histogram of results from data, non-spatial and spatial models, all with zero or negligible fade-out. (*a*, *b*) As in figure 6 ((*a*) all data, $n = 13$; (*b*) non-spatial simulations, $n = 71$). (*c*) Power ratios from twenty-year blocks with fade-out proportion less than the resolution limit from spatial simulations with $N = 5$, 10, 15 and $\phi = 10^{-4}$–10^{-1}. The spatial models capture (and indeed exaggerate) the long power-ratio tail observed in the data.

figure 8 shows a histogram of the power ratios of all data sets and non-spatial and spatial simulations with zero or negligible fade-out (cf. figure 6). Unlike the power ratios for the non-spatial simulations, the distribution of power ratios for the spatial simulations has a triennial tail similar to that of the distribution for the real data sets. In contrast to other ways of modifying the model to enhance persistence (section 3), spatial structure does not suppress three-year dynamics.

6. DISCUSSION AND CONCLUSIONS

Figure 8 represents a proof of plausibility; spatial structure can, under the right conditions, generate dynamics that simultaneously match the persistence and trienniality of some real data sets. As pointed out above, the correspondence between the spatially structured model and the real dynamics is not perfect; Copenhagen and Baltimore achieve epidemic peaks even higher than those of the non-spatial models, but have troughs similar to those of the spatially structured models.

The exact mechanism allowing spatially structured models to persist during triennial episodes is not clear. Examination of fade-out timing in different patches simply shows differences in phase among the patches that prevent all patches from going extinct simultaneously. Coupling is known to stabilize patch models (Hastings 1993), but there is no apparent reason why adding heterogeneity through a spatial stabilizing mechanism should differ from the various other mechanisms mentioned in section 3 in allowing triennial epidemics.

Some of the arguments for a spatial mechanism for measles persistence have pointed out that certain kinds

PHILOSOPHICAL TRANSACTIONS OF THE ROYAL SOCIETY B BIOLOGICAL SCIENCES

of spatial or social heterogeneity could help to maintain measles; for example, different schools or segments of the population could be affected by epidemics in different years, or there could be special isolated pools of susceptibles (e.g. in immigrant communities) who might be in particularly close contact with immigrating infectives. Similarly, microspatial structure – the detailed patterns of contact between children of different ages in interconnected families, neighbourhoods and school districts – may turn out to be more relevant than the broad spatial compartments used in our models. Heterogeneity at a small spatial scale would also allow apparent correlation at the scale of boroughs within a city or cities within a country while maintaining enough incoherence to preserve the persistence of measles. The simulations performed here give no information about the reality of any of these scenarios – only detailed data on the social and spatial distribution of cases during a real measles epidemic could do that. They do suggest that no such heterogeneities are necessary for a qualitative match between the persistence and dynamic properties of models and data, although extra structure might eliminate some of the remaining discrepancies between the data and the models.

The metapopulation models discussed here reduce the n^2 possible between-city contact parameters to one generic coupling parameter. It would be useful to be able to test a much wider class of models. In addition to heterogeneity in couplings between cities, there could be heterogeneity among cities in population size and effective density. Finally, there is no reason for spatial coupling to be constant by age and season; for example, children would probably have a lower cross-contact rate during the school term, but possibly a higher one during vacations. Preliminary results from models with heterogeneous spatial coupling and with age- and seasonally structured cross-couplings, suggest that there are not major qualitative differences between the simple metapopulation models considered here and more complex models.

Further research in this direction, however, is limited by computational and analytic ability. As the number of parameters and possible model structures increases combinatorially, it becomes more pressing to find new ways to estimate parameters for the models directly from the data. In addition, we need robust dynamically significant summaries of model behaviour that can be observed and tested against many aspects of the available data. The complex intermittent dynamics of seasonally driven measles models make many standard model validation tools inappropriate (Adkison 1992), but summaries such as fade-out proportion, power ratio, peak and trough incidence levels, internal correlation and fractions of cases in different age classes should help produce models that match the data in important ways. An extensive set of spatially and age-structured data on measles epidemics does exist (OPCS 1948–68), which may be suitable for refining the simple spatial models presented here.

As a final point, we note the rich episodic structure found in both models and case reporting data (figure 2*b*, *c*). These episodes have been linked to intermittency in models (Kendall *et al.* 1993; Schaffer *et al.* 1993) and to demographic shifts in the real world (Grenfell *et al.* 1993). Episodic dynamics may present an obstacle, generating non-stationary patterns and making it difficult to interpret the underlying causes of dynamic changes; alternatively, we can interpret them as an opportunity, allowing the possibility of linking another supposed dynamic curiosity with a real epidemiological system.

Persistence and epidemic cycles have traditionally been studied as separate aspects of epidemiology. This study shows that, at least for measles epidemics, persistence and cyclic dynamics are tightly linked. The probability of fade-out depends inevitably on the pattern of recurrent epidemics, and vice versa. In addition, models show that spatial structure has the potential to alter persistence and the association between persistence and dynamics significantly. However, to *prove* the importance of spatial structure, and to match the spatial dynamics of the models with data, there will be no substitute for more careful analysis of spatially structured measles data.

This research was partly completed with the support of the Paul Mellon Fellowship (B.B.) and the Isaac Newton Institute for Mathematical Sciences. We thank Jonathan Dushoff for a number of useful suggestions.

REFERENCES

Adkison, M. 1992 Parameter estimation for models of chaotic time-series. *J. math. Biol.* **30**, 839–852.

Adler, F. & Nuernberger, B. 1994 Persistence in patchy irregular landscales. *Theor. Popul. Biol.* **45**(1), 41–75.

Anderson, R. & May, R. 1984 Spatial, temporal, and genetic heterogeneity in host populations and the design of immunization programmes. *IMA J. Math. Appl. Med. Biol.* **1**, 233–266.

Anderson, R.M. & May, R.M. 1985*a* Age-related changes in the rate of disease transmission: implications for the design of vaccination programmes. *J. Hyg., Camb.* **94**, 365–436.

Anderson, R.M. & May, R.M. 1985*b* Age-related changes in the rate of disease transmission: implications for the design of vaccination programmes. *J. Hyg., Camb.* **94**, 365–436.

Anderson, R.M. & May, R.M. 1986 The invasion, persistence and spread of infectious diseases within animal and plant communities. *Phil. Trans. R. Soc. Lond.* B **314**, 533–570.

Anderson, R.M. & May, R.M. 1992 *Infectious diseases of humans: dynamics and control*. Oxford University Press.

Aron, J. & Schwartz, I.B. 1984 Seasonality and period-doubling bifurcations in an epidemic model. *J. theor. Biol.* **110**, 665–679.

Bartlett, M.S. 1957 Measles periodicity and community size. *Jl R. statist. Soc.* A **120**, 48–70.

Bartlett, M.S. 1960*a* The critical community size for measles in the U.S. *Jl R. statist. Soc.* A **123**, 37–44.

Bartlett, M.S. 1960*b* *Stochastic population models in ecology and epidemiology*. London: Methuen.

Becker, N. & Wang, D. 1993 *Severe outbreak of measles in an isolated German village, 1861. II: analysis of transmission rates.*

Berryman, A. & Millstein, J. 1989 Are ecological systems chaotic – and if not, why not? *Trends Ecol. Evol.* pp. 26–28.

Black, F. 1966 Measles endemicity in insular populations:

PHILOSOPHICAL TRANSACTIONS OF THE ROYAL SOCIETY B BIOLOGICAL SCIENCES

critical community size and its evolutionary implication. *J. theor. Biol.* **11**, 207–211.

Boccara, N. & Cheong, K. 1992 Automata network SIR models for the spread of infectious diseases in populations of moving individuals. *J. Phys.* A **25**(9), 2447–2461.

Boccara, N. & Cheong, K. 1993 Critical behavior of a probabilistic automata network SIS model for the spread of an infectious disease in a population of moving individuals. *J. Phys.* A **26**(15), 3707–3717.

Bolker, B.M. 1993*a* Chaos and complexity in measles models: a comparative numerical study. *IMA J. Math. Appl. Med. Biol.* **10**, 83–95.

Bolker, B.M. 1993*b* Dynamics of measles epidemics in developed countries. Ph.D. thesis, Cambridge University.

Bolker, B.M. & Grenfell, B.T. 1993 Chaos and biological complexity in measles dynamics. *Proc. R. Soc. Lond.* B **251**, 75–81.

Chatfield, C. 1975 *The analysis of time series: theory and practice.* London: Chapman and Hall.

Cliff, A.D. & Haggett, P. 1988 *Atlas of disease distributions: analytical approaches to epidemiological data.* Oxford: Basil Blackwell.

Ellner, S., Gallant, A. & Theiler, J. 1993 Detecting nonlinearity and chaos in epidemic data. In *Epidemic models: their structure and relation to data* (ed. D. Mollison), pp. 229–247. Cambridge University Press.

Engbert, R. & Drepper, F. 1995 Qualitative analysis of unpredictability: a case study from childhood epidemics. In *Proc. nonlin. Sci.* Wiley. (In the press.)

Fine, P.E.M. & Clarkson, J.A. 1982*a* Measles in England and Wales – I: an analysis of factors underlying seasonal patterns. *Int. J. Epid.* **11**, 5–15.

Fine, P.E.M. & Clarkson, J.A. 1982*b* Measles in England and Wales – II: the impact of the measles vaccination programme on the distribution of immunity in the population. *Int. J. Epid.* **11**, 15–25.

Grebogi, C., Ott, E. & Yorke, J. 1983 Crises, sudden changes in chaotic attractors, and transient chaos. *Physica* D 181–200.

Grenfell, B.T. 1992 Chance and chaos in measles dynamics. *Jl R. statist. Soc.* B **54**, 383–398.

Grenfell, B.T., Bolker, B. & Kleczkowski, A. 1993 Seasonality, demography, and the dynamics of measles in developed countries. In *Epidemic models: their structure and relation to data* (ed. D. Mollison), pp. 248–268. Cambridge University Press.

Grenfell, B.T., Kleczkowski, A., Ellner, S. & Bolker, B. 1995 Measles as a case study in nonlinear forecasting and chaos. *Phil. Trans. R. Soc. Lond.* A **348**, 515–530.

Griffiths, D. 1973 The effect of measles vaccination on the incidence of measles in the community. *Jl R. statist. Soc.* A **136**, 441–449.

Hassell, M., Comins, H. & May, R. 1991 Spatial structure and chaos in insect population dynamics. *Nature, Lond.* **353**, 255–258.

Hastings, A. 1993 Complex interactions between dispersal and dynamics: lessons from coupled logistic equations. *Ecology* **74**(5), 1362–1372.

Hilborn, R. 1975 The effect of spatial heterogeneity on the persistence of predator–prey interactions. *J. theor. Biol.* **8**, 346–355.

Huffaker, C. 1958 Experimental studies in predation: dispersion factors and predator–prey interactions. *Hilgardia* **27**, 343–383.

Kalivianakis, M., Mous, S.L. & Grasman, J. 1995 Reconstruction of the seasonally varying contact rate for measles. *Math. Biosci.* **124**, 225–234.

Kendall, B., Schaffer, W. & Tidd, C. 1993 Transient periodicity in chaos. *Phys. Lett.* A **177**, 13–20.

Kleczkowski, A. & Grenfell, B.T. 1995 *Cellular automata model of epidemic spread with an application to measles dynamics in developed countries.* (In preparation.)

May, R.M. & Anderson, R.M. 1984 Spatial heterogeneity and the design of immunization programs. *Math. Biosci.* **72**, 83–111.

Murray, G. & Cliff, A.D. 1975 A stochastic model for measles epidemics in a multi-region setting. *Inst. Br. Geog.* **2**, 158–174.

Nychka, D., Ellner, S., Gallant, A. & McCaffrey, D. 1992 Finding chaos in noisy systems. *Jl R. statist. Soc.* B **54**, 399–426.

Olsen, L. & Schaffer, W. 1990 Chaos versus noisy periodicity: alternative hypotheses for childhood epidemics. *Science, Wash.* **249**, 499–504.

Olsen, L., Truty, G. & Schaffer, W. 1988 Oscillations and chaos in epidemics: a nonlinear dynamic study of six childhood diseases in Copenhagen, Denmark. *Theor. Popul. Biol.* **33**, 344–370.

OPCS 1948–68 *Registrar General's weekly reports, England and Wales.* London: H.M.S.O. (British government summaries of infectious disease case reports, produced by the Office of Population Censuses and Surveys).

Pimental, D., Nagel, W. & Madden, J. 1963 Space–time structure of the environment and the survival of parasite–host systems. *Am. Nat.* **97**, 141–167.

Rand, D. & Wilson, H. 1991 Chaotic stochasticity: a ubiquitous source of unpredictability in epidemics. *Proc. R. Soc. Lond.* B **246**, 179–184.

Sattenspiel, L. & Dietz, K. 1995 A structured epidemic model incorporating geographic mobility among regions. *Math. Biosci.* (In the press.)

Schaffer, W., Kendall, B., Tidd, C. & Olsen, L. 1993 Transient periodicity and episodic predictability in biological dynamics. *IMA J. Math. Appl. Med. Biol.* **10**(4), 227–247.

Schenzle, D. 1984 An age-structured model of pre- and post-vaccination measles transmission. *IMA J. Math. Appl. Med. Biol.* **1**, 169–191.

Schwartz, I.B. 1985 Multiple stable recurrent outbreaks and predictability in seasonally forced nonlinear epidemics. *J. math. Biol.* **21**, 347–361.

Schwartz, I.B. 1992 Small amplitude, long period outbreaks in seasonally driven epidemics. *J. math. Biol.* **30**, 473–491.

Shaw, D. 1990 An initial exploration of the course of measles epidemics in England and Wales from 1960 to 1963. Undergraduate thesis, Sheffield University.

Smith, H. 1983 Subharmonic bifurcation in an S–I–R epidemic model. *J. math. Biol.* **17**, 163–177.

Soper, M. 1929 The interpretation of periodicity in disease prevalence. *Jl R. statist. Soc.* A **92**, 34–61.

Stone, L. 1992 Coloured noise or low-dimensional chaos. *Proc. R. Soc. Lond.* B **250**, 77–81.

Stone, L. 1993 Period-doubling reversals and chaos in simple ecological models. *Nature, Lond.* **365**, 617–620.

Sugihara, G. & May, R.M. 1990 Nonlinear forecasting as a way of distinguishing chaos from measurement error in time series. *Nature, Lond.* **344**, 734–741.

Sugihara, G., Grenfell, B.T. & May, R.M. 1990 Distinguishing error from chaos in ecological time series. *Phil. Trans. R. Soc. Lond.* B **330**, 235–251.

Tidd, C., Olsen, L. & Schaffer, W. 1993 The case for chaos in childhood epidemics. 2: Predicting historical epidemics from mathematical models. *Proc. R. Soc. Lond.* B **254**, 257–273.

(*Received 6 September 1994; accepted 4 November 1994*)

PHILOSOPHICAL TRANSACTIONS OF THE ROYAL SOCIETY B BIOLOGICAL SCIENCES